Anal. Chem. **2001,** *73,* 3521−3527

Articles

Molecular Oxygen-Sensitive Fluorescent Lipobeads for Intracellular Oxygen Measurements in Murine Macrophages

Jin Ji,[†] Nitsa Rosenzweig,[‡] Imanie Jones,[‡] and Zeev Rosenzweig*[,†]

Department of Chemistry, University of New Orleans, New Orleans, Louisiana 70148, and Department of Chemistry, Xavier University of Louisiana, New Orleans, Louisiana 70125

Intracellular oxygen concentration is of primary importance in determining numerous physiological and pathological processes in biological systems. This paper describes the development and application of micrometer-sized oxygen-sensitive fluorescence lipobeads for intracellular measurements of molecular oxygen in J774 murine macrophages. A ruthenium diimine complex $[Ru(bpy\text{-}pyr)(bpy)_2]Cl_2$ (bpy = 2,2′-bipyridine, bpy-pyr = 4-(1″-pyrenyl)-2,2′-bipyridine) is used as the oxygen indicator. The indicator exhibits high chemical and photostability and high sensitivity to oxygen. The indicator molecules are immobilized in a phospholipid membrane that coats polystyrene microparticles. The fluorescence of the lipobeads is effectively quenched by molecular oxygen. The fluorescence intensity of the oxygen-sensitive lipobeads is 3 times higher in a nitrogenated solution than in an oxygenated solution. The lipobeads are internalized by murine macrophages through phagocytosis. They maintain their spectral properties for 24 h in living cells when the cells are stored in phosphate-buffered saline at pH 7.4. The photostability, reversibility, and effect of hypoxia, hyperoxia, and oxidative stress on the intracellular level of oxygen in J774 murine macrophages are described.

Intracellular oxygen concentration is a key indicator of numerous physiological and pathological processes in biological systems. In cells, excess oxygen leads to overproduction of the extremely reactive and unstable reactive oxygen species (ROS), which oxidize lipids, carbohydrates, DNA, and proteins, altering their structure and function.[1,2] The determination of oxygen concentration is of particular importance in tumor cells since it may enable the prediction of the response of the tumor to radiation and chemotherapy.[3−5] The development of a real-time measurement technique for the determination of intracellular oxygen concentrations would be highly valuable for studies aiming to reveal how oxygen imbalance affects normal and cancerous cells.

Despite the significance of intracellular oxygen in various biochemical processes, there are surprisingly few analytical methods to measure its levels.[6,7] The role of oxygen in cellular processes is mostly assessed by indirect data derived from the measurement of extracellular oxygen concentration. This approach is ambiguous, as there is a difference between intracellular and extracellular oxygen concentrations.[8,9] Clark electrodes have been widely used to measure extracellular oxygen levels in cell culture media.[6,10] However, when applied to intracellular studies, the electrodes may cause structural damage to the cell membrane due to penetration. The use of oxygen microelectrodes only enables the measurement of molecular oxygen in one cell at a time and is not suitable for applications that require fast cell screening. Furthermore, the technique often gives misleading information due to the abundance of interfering species in the cytoplasm. The consumption of oxygen by the electrodes can alter the cellular oxygen level near the electrode and lead to false readings as well.

Nuclear magnetic resonance (NMR) spectroscopy provides a noninvasive method for intracellular oxygen concentration measurements.[5,11] However, in NMR, the concentration of oxygen is analyzed indirectly from measurements of oxygen-dependent metabolic species. The technique is limited in temporal resolution due to the relatively long relaxation time of biologically relevant nuclei and in spatial resolution due to the size of NMR probes.

[†] University of New Orleans.
[‡] Xavier University of Louisiana.

(1) Tortora, G.; Funke, B.; Case, C. L. *Microbiology*, 5th ed.; The Benjamin/Cummings Publishing Co. Inc.: Reading, MA, 1995; pp 413−414.
(2) Martinez-Cayuela, M. *Biochimie* **1995**, *77*, 7−161.
(3) Lo, Y. Y.; Cruz, T. F. *J. Biol. Chem.* **1995**, *270* (20), 11727−11730.
(4) McIlroy, B. W.; Curnow, A.; Buonaccorsi, G.; Scott, M. A.; Brown, S. G.; MacRobert, A. *J. Photochem. Photobiol. B: Biol.* **1998**, *43*, 47−55.
(5) Glickson, J. J., Wehrle, J. P., Rajan, S. S., Li, S. J., Steen, R. G., Pettegrew, J. W., Eds. NMR spectrocscopy of tumors. In *NMR: Principles and Applications to Biomedical Research;* Springer-Verlag: New York, 1990; pp 255−309.
(6) Lau, Y. Y.; Abe, T.; Ewing, A. G. *Anal. Chem.* **1992**, *64* (15), 1702−1705.
(7) Chen, K.; Ng, C. E.; Zweier, J. L.; Kuppusamy, P.; Glickson, J. D.; Swartz, H. M. *Magn. Reson. Med.* **1994**, *31* (6), 668−672.
(8) Robiolio, M.; Rumsey, W. L.; Wilson, D. F. *Am. J. Physiol.* **1989**, *256* (6 pt 1), C1207−1213.
(9) Glockner, J. F.; Swartz, H. M.; Pals, M. A. *J. Cell. Physol.* **1989**, *140* (3), 505−511.
(10) Titovets, E. *Anal. Biochem.* **1987**, *166* (1), 79−82.
(11) Long, R. C.; Papas, K. K.; Sambanis, A.; Constantinidis, I. *J. Magn. Reson.* **2000**, *146* (1), 49−57.

10.1021/ac010344n CCC: $20.00
Published on Web 07/04/2001

Electron spin resonance (ESR) spectroscopy has also been used for intracellular and extracellular oxygen measurements.[12−15] This technique is based on the interaction between molecular oxygen and paramagnetic materials such as nitroxides. Oxygen broadens the ESR spectral lines of paramagnetic probes via Heusenberg spin exchange in a concentration-dependent manner. The use of these paramagnetic probes combined with recent instrumental developments extends the use of ESR to large water-containing specimens and enables the measurement of oxygen in the same type of samples used for NMR studies of cells. However, the technique is susceptible to electromagnetic interference and lacks real-time measurement capability.

Fluorescence microscopic techniques have been used widely for the measurement of pH and ion levels in single cells.[16,17] The measurements are based on the interaction of fluorophors with the ions of interest, which results in a concentration-dependent change in their fluorescence intensity. Recently, we reported the use of the fluorophore tris(1,10-phenanthroline)ruthenium chloride ($Ru(phen)_3$) for the measurement of the effect of external hypoxia on the molecular oxygen level in J774 murine macrophages. The measurement was based on the fluorescence quenching of $Ru(phen)_3$ by molecular oxygen. However, these measurements had limited sensitivity due to instability of the fluorescence intensity of $Ru(phen)_3$ in the cellular environment. A continuous negative signal drift observed in these experiments was attributed to the interaction of $Ru(phen)_3$ with cellular components such as proteins, DNA, and ROS. Fiber-optic oxygen sensors have also been fabricated for oxygen measurements in cells.[18,19] In these sensors, the fluorescence indicator is immobilized in a polymer matrix that is attached covalently to the distal end of the fiber. The polymer matrix protects the dye from the effect of intracellular macromolecules and ROS. Unlike oxygen electrodes, fiber-optic oxygen sensors do not consume oxygen during measurements. However, invasion or penetration of the sensor into the observed cell still occurs and structural damage to the cell membrane is a concern. Similarly to electrodes, the application of fiber-optic oxygen sensors for cellular analysis has been also limited by their low throughput.

To overcome the low throughput of electrodes and fiber-optic sensors, Kopelman et al. developed a new type of nanosensor named PEBBLEs (*p*robes *e*ncapsulated *b*y *b*iologically *l*ocalized *e*mbedding). PEBBLEs (ranging from 20 to 200 nm in diameter) were fabricated and applied for intracellular measurements of pH, molecular oxygen, calcium ions, glucose, and nitric oxide in single cells.[20−22] These new nanosensors show very high selectivity and reversibility, fast response time, and reversible analyte detection. They are delivered into the observed cells by a variety of minimally invasive techniques, including picoinjection, gene gun delivery, liposomal incorporation, and natural ingestion. The new technique offers several important advantages. First, as in cellular labeling techniques, chemical information can be obtained from a large number of cells simultaneously. Second, because of their small size the particles can be used to detect analytes in cellular organelles. Third, the technique is truly noninvasive, allowing intracellular measurements while maintaining cellular viability. Last, embedding the fluorescence sensing dyes in the PEBBLEs avoids dye compartmentalization and enables the differentiation of the nanosensor location from autofluorescence centers in the observed cells. However, PEBBLE-based fluorescence sensors have some structural problems that limit their quantitative power. Hydrophobic particles do not disperse in aqueous samples and tend to aggregate. As a result, hydrophilic PEBBLEs, where the sensing indicator is embedded in hydrophilic polymers, e.g., hydrogels, have been prepared and used to measure analyte levels in aqueous samples and cells. This approach limits the sensing technique to hydrophilic indicators. Furthermore, unless the indicators are covalently bound to the polymer network, a high leaking rate is expected, which decreases the stability and sensitivity of the sensor.

Recently we reported the synthesis and application of micrometric phospholipid-coated polystyrene particles named lipobeads as intracellular pH sensors.[23,24] In lipobeads, the sensor is composed of a polymer particle coated with a phospholipid membrane. The fluorescence-sensing molecules are immobilized in the membrane. The interaction between the dye and cellular components is minimized, as well as the toxicity of the dye. This paper describes the preparation, characterization, and application of oxygen-sensitive lipobeads for real-time intracellular oxygen measurements in J774 murine macrophages. A highly hydrophobic ruthenium metal complex, $Ru(bpy\text{-}pyr)(bpy)_2$, (bpy = 2,2′-bipyridine, bpy-pyr = 4-(1″-pyrenyl)-2,2′-bipyridine) is used as the oxygen indicator.[24] The indicator displays strong emission via metal-to-ligand charge transfer (MLCT) with an excited-state lifetime of 1.3 μs. It exhibits a high molar absorption coefficient of $2 \times 10^4\ M^{-1}\ cm^{-1}$ at 456 nm and an emission quantum yield of 0.1 at 632 nm, which presents a preferable large Stoke shift. The oxygen-sensitive lipobeads show significant improvement in stability and biocompatibility compared to previously used sensors in intracellular studies. The analytical properties of the lipobeads and their application for oxygen measurements in murine macrophages under conditions of hypoxia, hyperoxia, and oxidative stress are discussed.

EXPERIMENTAL SECTION

Digital Fluorescence Microscopy. The experimental setup used for fluorescence measurements of the oxygen-sensitive

(12) Glockner, J.; Norby, S. W.; Swartz, H. M. *Magn. Reson. Med.* **1993**, *29* (1), 12−18.
(13) Santini, M. T., Morelli, G.; Fattorossi, A.; Malorni, W.; Rainaldi, G.; Indovina, P. L. *Free Radical Biol. Med.* **1996**, *20* (7), 915−924.
(14) Povich, M. J. *Anal. Chem.* **1975**, *47* (2), 346−347.
(15) Lai, C. S.; Hopwood, L. E.; Hyde, J. S.; Lukiewicz, S. *Proc. Natl. Acad. Sci. U.S.A.* **1982**, *79* (4), 1166−1170.
(16) Radosevic K.; de Grooth, B. G.; Greve, J. *Cytometry* **1995**, *20* (4), 281−289.
(17) Muallem, S.; Zhang, B. X.; Loessberg, P. A.; Star, R. A. *J. Biol. Chem.* **1992**, *267* (25), 17658−17664.
(18) Stefansson, E.; Peterson, J. I.; Wang, Y. H. *Am. J. Physiol.* **1989**, *256* (4 Pt 2), H1127−1133.
(19) Zhao, Y.; Richman, A.; Storey, C.; Radford, N. B.; Pantano, P. *Anal. Chem.* **1999**, *71*, 3887−3893.
(20) Clark, H. A.; Marion, H.; Martin, A. P.; Kopelman, R. *Anal. Chem* **1999**, *71*, 4831−4836.
(21) Clark, H. A.; Kopelman, R.; Tjalkens, R.; Philbert, M. *Anal. Chem* **1999**, *71*, 4837−4843.
(22) Clark, H. A.; Barker, S. L. R.; Brasuel, M.; Miller, M. T.; Monson, E.; Parus, S.; Shi, Z. Y.; Song, A.; Thorsrud, B.; Kopelman, R.; Ade, A.; Meixner, W.; Athey, B.; Hoyer, M.; Hill, D.; Lightle, R.; Philbert, M. A. *Sens. Actuators B* **1998**, *51*, 12−16.
(23) McNamara, K. P.; Rosenzweig, N.; Rosenzweig, Z. *Proc. SPIE BiOS 2000 Symp.* **2000**, *3922*, 148−157.
(24) Simon, J. A.; Curry, S. L.; Schmehl, R. H.; Schatz, T. R.; Piotrowiak, P.; Jin, X. Q.; Thummel, R. P. *J. Am. Chem. Soc.* **1997**, *119*, 11012−11022.

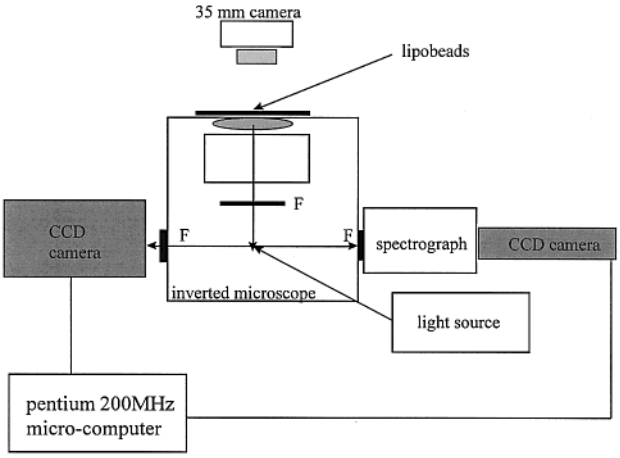

Figure 1. Digital fluorescence imaging microscopy system. The experimental setup consists of an inverted fluorescence microscope with a 20× or 40× objective (NA = 0.5 or 0.9) and a high-performance charge-coupled device camera (16-bit resolution, 512 × 512 chip size). A PC-compatible microcomputer equipped with digital imaging analysis (Winview 3.2, Roper Scientific) is used for data analysis.

lipobeads is shown in Figure 1. The system consists of an inverted fluorescence microscope (Olympus IX-70) equipped with three detection ports. A 100-W mercury lamp is used as the light source for excitation. The fluorescence is collected by a 20× or 40× microscope objective with a numerical aperture 0.5 or 0.9, respectively. A filter cube containing a 480-nm narrow band excitation filter, 500-nm dichroic mirror, and 515-nm long-pass emission filter is used to ensure spectral purity. A high-performance charge-coupled device (CCD) camera (Rupert Scientific, model 256HB) with a 512 × 512 pixel array is used for digital fluorescence imaging of the samples. The Rupert Scientific software Winview 3.2 is used for image analysis.

Synthesis of Oxygen-Sensitive Lipobeads. Four milligrams of polystyrene microspheres is dispersed in 100 μL of ethanol/hexane (v/v 1:1) mixture by sonication using a 47-kHz, Bransonic sonicator. A lipid stock solution (50 mM) is prepared with a 5:4:1 molar ratio of dimyristoylphosphatidylcholine, cholesterol, and dihexadecyl phosphate in chloroform. A 100-μL aliquot of of 0.1 mM $[(bpy)_2Ru(bpy\text{-}pyr)]Cl_2$ in $CHCl_3$ is added to the lipid solution. The solution is briefly vortexed to ensure homogeneity. A 100-μL aliquot of the microsphere suspension is then slowly added while the mixture is sonicated in an ice bath. The solution is kept at room temperature for 1 h to allow the indicator and the phospholipid molecules to absorb onto the surface of the particles. The sample is then dried overnight under nitrogen. The dried beads are resuspended in 1 mL of phospahte-buffered saline (PBS) solution at pH 7.4. The lipobeads solution is sonicated for 30 min in an ice bath to break formed aggregates, remove loosely bound indicator molecules, and ensure even phospholipid coating of the particles. Excess phospholipids, indicator, and uncoated beads are removed by centrifugation (1000*g*, 15 min). Lipobeads evenly coated with indicator and phospholipids are collected at the bottom of the glass centrifuge tube while the supernatant and floating beads are decanted. The low-speed centrifugation is necessary to minimize leakage of the indicator from lipobeads. The lipobeads are resuspended and stored in 2 mL of PBS (pH 7.4) at 4 °C. Under these storage conditions, the lipobeads maintain their oxygen sensitivity for at least two weeks.

Photostability Measurements of Ru(bpy-pyr)(bpy)$_2$. Solutions of $Ru(bpy\text{-}pyr)(bpy)_2$ and $Ru(phen)_3$ were continuously exposed to a 765-W xenon lamp in a Sunbox (Suntest CPS$^+$, Atlas Electric Devices Co.). The fluorescence intensity of the solutions was acquired every 5 min using a spectrofluorometer (PTI, Quantmaster).

Immobilization of Lipobeads on the Surface of a Chambered Cover Glass for Calibration Measurements. To immobilize the lipobeads, a chambered cover glass (borosilicate, Nalge Nunc International) is rinsed with 70% ethanol/water, followed by a thorough wash with deionized water. The chambered cover glass is incubated overnight in a 200-μL solution of 0.01% poly(L-lysine). It is then rinsed with deionized water and PBS solution at pH 7.4. A 200-μL lipobead suspension is then placed in the chambered cover glass for 1 h. The unimmobilized lipobeads are then rinsed out with a PBS solution at pH 7.4.

Cell Culture. Cultures of J774 murine macrophages are maintained according to a protocol described by Gordon et al.[25] The cells are cultured in Dulbecco's modified Eagle's medium supplemented with 4 mM L-glutamine, 1.5 g/L sodium bicarbonate, 4.5 g/L glucose, 1.0 mM sodium pyruvate, and 10% fetal bovine serum. The cells are grown at 37 °C under 5% CO_2. The medium is replaced three times a week. To prepare subcultures, the cells are scraped in new medium and split into new plates.

Cell Culture on the Surface of a Chambered Cover Glass. The macrophages are detached from the surface of a tissue culture plate by scraping. The cells are mixed with the growth medium by a glass pipet. A 5-μL aliquot of the cell suspension ($\sim 1 \times 10^6$ cells/mL) is then placed in a chambered cover glass. A total of 950 μL of fresh medium is added to the chamber. The cells are incubated to attach and grow on the chambered cover glass at 37 °C under 5% CO_2. Typically 80% confluency is achieved in 3 days.

Phagocytosis of Lipobeads by Macrophages. A solution of 150 μL of medium containing 0.5 mg/mL lipobeads is briefly sonicated and added to a chambered cover glass covered with cells at 80% confluence. The cells are incubated with the lipobead suspension at room temperature for 1 h to allow the phagocytosis of lipobeads to take place. The excess lipobeads are washed out with PBS solution at pH 7.4.

Materials and Reagents. Trisbipyridine-4-(1′′′′-pyrenyl)-2,2′-bipyridineruthenium chloride ($Ru(bpy\text{-}pyr)(bpy)_2]Cl_2$) was a gift from Dr. Russell Schmehl of Tulane University. $Ru(phen)_3$ was purchased from Aldrich. 1,2-Dimyristoyl-*sn*-glycero-3-phosphocholine (DMPC) was purchased from Avanti Polar Lipids. Glucose, glucose oxidase from *Aspergillus niger* with enzymatic activity of 10 000 units/mL, 0.1% poly(L-lysine), menadione, Dulbecco's modified Eagle's medium, and bovine serum albumin were purchased from Sigma. J774 murine macrophages were purchased from American Type Culture Collection (ATCC). Lab-Tek II chambered cover glass used for microscopy and pH buffers were purchased from Fisher Scientific. Aqueous solutions were prepared with a 18-MΩ deionized water purification system (Barnstead Thermolyne Nanopure). PBS solutions at pH 7.4 were prepared from PBS tablets (Amresco). All reagents were used as received without further purification.

(25) Gordon, S. *BioEssays* **1995**, *17* (11), 977−986.

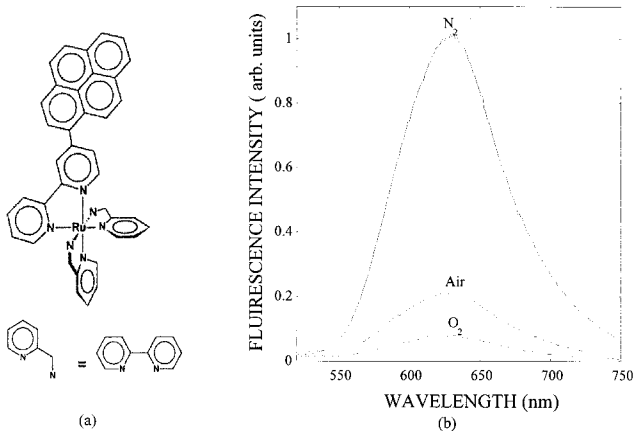

Figure 2. (a) Structure of Ru(bpy-pry)$(bpy)_2$. bpy = 2,2′-bipyridine, bpy-pyr = 4-(1″-pyrenyl)-2,2′-bipyridine). (b) Response of free [(bpy)-2Ru(bpy-pry)] to different oxygen levels in PBS at pH 7.4. The experiments are conducted in a spectrofluorometer.

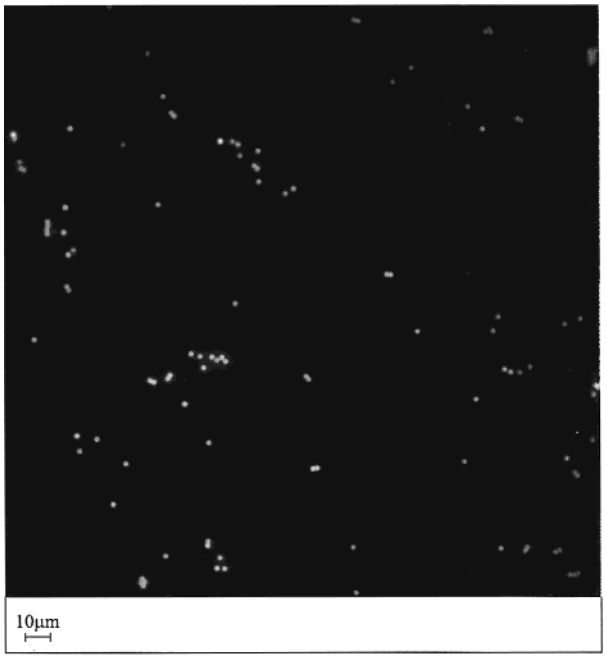

Figure 3. Digital fluorescence image of 2.1-μm oxygen-sensitive lipobeads: Light source, 100-W mercury lamp; excitation filter, D480/30X; dichroic mirror, 500 nm; emission filter, BA 515 nm; objective:, 20× with NA = 0.5; neutral density, 1.0; exposure time, 0.5 s. The imaging conditions remain the same through the experiments unless otherwise stated.

RESULTS AND DISCUSSION

Choice of Indicator. Ru(II)$(L)_3^{2+}$ complexes (L = 2,2′-bipyridine, 1,10-phenanthroline, or substituted derivatives) have been used frequently as indicators for oxygen level determination in gas samples and aqueous solutions due to their strong visible absorption, high photochemical stability, high fluorescence quantum yield, and relatively long excited-state lifetimes. However, most of these complexes are hydrophilic. We have previously prepared and used lipobeads containing tris(1,10-phenanthroline)-ruthenium chloride for oxygen measurements in aqueous samples. However, because of the high leaking rate of Ru$(phen)_3$ from the lipobeads, the sensors show poor stability. In this study, a ruthenium(II) diimine−pyrene complex, Ru(bpy-pyr)$(bpy)_2$ (structure shown in Figure 2a), is used for the first time as an oxygen indicator for cellular oxygen measurements. In addition to the strong visible absorption, high photochemical stability, efficient fluorescence, and relatively long-lived MLCT excited state, this indicator is hydrophobic and has low solubility in aqueous solutions. It adsorbs strongly to the membrane of the lipobeads, showing insignificant leakage rate during two weeks storage in PBS solution at pH 7.4. Figure 2b shows the fluorescence spectra of Ru(bpy-pyr)$(bpy)_2$ in nitrogen, air, and oxygen-saturated solutions. Due to dynamic quenching by molecular oxygen, the fluorescence intensity of Ru(bpy-pyr)$(bpy)_2$ in a nitrogen-saturated solution is 13 times higher than the fluorescence of the dye in an oxygen-saturated solution. The dependence of the fluorescence intensity of the dye on the concentration of dissolved oxygen is determined by the Stern−Volmer equation.[26] The indicator responds more efficiently to a lower range of oxygen concentration.

Formation of Lipobeads. The phospholipid-coated polystyrene beads, lipobeads, are formed through physical adsorption. When a hydrophobic dye such as Ru(bpy-pyr)$(bpy)_2$ is added to the lipobead suspension, the dye molecules are trapped in the hydrophobic regions of the phospholipid membrane coating of the particles. The phospholipid membrane formed on the surface of the polystyrene core is not only biocompatible but also provides protection for the sensing fluorophore from the intercellular environment. Interaction between the dye and proteins is minimized, as well as intracellular sequestration and toxicity of the dye. A digital fluorescence image of fluorescent lipobeads averaging 2.1 μm in diameter is shown in Figure 3. It can be seen that the lipobeads are evenly coated with the indicator and exhibit bright fluorescence with a signal-to-noise ratio of 20. Photostability study of the new indicator is conducted by comparing its photobleaching property with that of the highly photostable Ru-$(phen)_3$ complex. The two dyes are exposed to a 765-W senon lamp in a Sunbox continuously for 1 h. Both dyes show a 50% fluorescence decrease in 30 min of continuous exposure to light (data not shown). The photobleaching rates are comparable. To minimize the photobleaching rate of the dye and the effect of cellular autofluorescence, excitation light at the nonoptimum excitation wavelength of 480 nm is used for oxygen measurements instead of the optimum excitation wavelength of 460 nm. Additionally, a neutral density filter of 1.0 is used to reduce the excitation intensity of the 100-W mercury light source. We also limit the exposure time to 0.5 s and the number of exposures during kinetic measurements to 20 in order to protect the fluorescent lipobeads from photobleaching. Under these conditions, the lipobeads are photostable during experiments that last up to 1 h.

Analytical Properties of the Oxygen-Sensitive Lipobeads in Aqueous Solution. The fluorescence intensity of the lipobeads is ∼3 times higher in nitrogenated solutions than in oxygenated ones. The analytical range of the lipobeads is governed by the respective quenching curve and the Stern−Volmer constant. The variation in the fluorescence intensity as a function of dissolved oxygen concentration is given by the Stern−Volmer equation: $I_0/I_c = 1 + K_{sv}[O_2]$, where I_0 is the fluorescence intensity of Ru(bpy-

(26) Stern, O.; Volmer, M. *Z. Phys.* **1919**, *20*, 183−189.

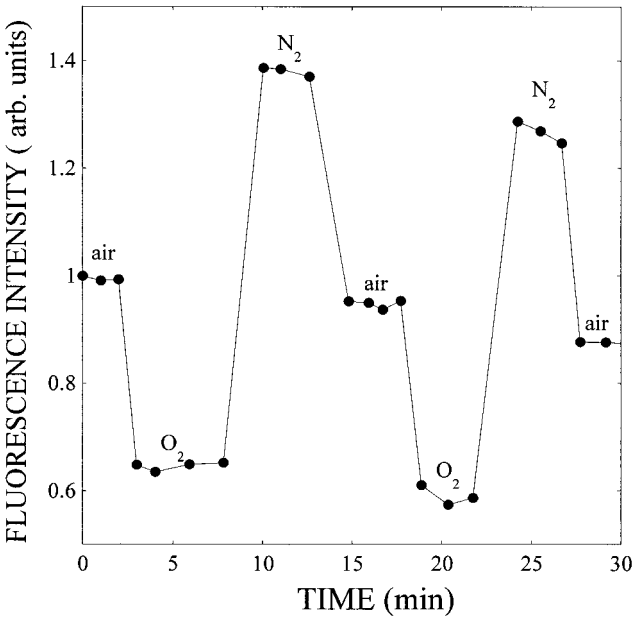

Figure 4. Reversibility of oxygen-sensitive Ru(bpy-pry)$(bpy)_2$-containing lipobeads. The lipobeads are repeatedly exposed to oxygenated or nitrogenated solutions. The experiments are conducted using a digital fluorescence microscopy system.

pyr)bpy_2 in a nitrogenated solution, I_c is the fluorescence intensity of Ru(bpy-pyr)bpy_2 in a solution of given dissolved oxygen concentration, and K_{sv} is the Stern−Volmer quenching constant. In principle, higher quenching constants result in higher accuracy at low levels of oxygen. This is due to the larger signal change per oxygen concentration interval. However, high quenching constants result in a more limited linear dynamic range. K_{sv} for Ru(bpy-pyr)$(bpy)_2$ containing lipobeads is 4730 ± 5% M^{-1}. The linear dynamic range is between 0.1 and 12 ppm molecular oxygen with a correlation coefficient of 0.991. We found a standard deviation of ∼4% between 10 consecutive fluorescence measurements in air-saturated solutions. The standard deviation increases at high oxygen levels where the signal is low up to 10%. To test the reversibility of the lipobeads, lipobeads are immobilized on the surface of a chambered cover glass coated with poly(L-lysine). The lipobeads are then exposed to oxygen-, air-, and nitrogen-saturated solutions repeatedly. Figure 4 describes the fluorescence intensity, normalized to the fluorescence intensity in air-saturated solution, of the immobilized lipobeads. The fluorescence of the lipobeads decreases by ∼40% when the cells are incubated in an oxygen-saturated PBS solution, indicating an increase of the oxygen level over 12 ppm, the upper linear limit of the lipobead-based sensor. The fluorescence of the lipobeads increases instantly by 2.5-fold when the oxygenated buffer is replaced with a nitrogenated PBS solution. Replacing the nitrogenated solution with an air-saturated solution restores the fluorescence signal to its original level. It can be seen that the oxygen-sensing lipobeads are reversible and their response and recovery times are in the seconds time scale.

Intracellular Oxygen Measurements Using Oxygen-Sensing Lipobeads. The lipobeads are applied to monitor intracellular oxygen level changes in J774 murine macrophages. Lipobeads are internalized by the macrophages and directed to intracellular lysosomes through phagocytosis. A bright-field image and a digital fluorescence image taken through a 40× microscope objective of the lipobeads internalized by macrophages are shown in Figure 5. The lipobeads maintain their structural integrity, spectral properties, and oxygen sensitivity for over 24 h following phagocytosis. When the cells are exposed to extreme conditions of hyperoxia or hypoxia, they appear to resist the rapid gas diffusion before they are overwhelmed. However, such treatment leads to irreversible changes in the physical shape of the cells and eventually to cell death as confirmed by a standard Trypan Blue staining method.

To test the sensitivity of the lipobeads under less destructive conditions, we applied the oxygen-sensitive lipobeads to monitor the cellular response of individual macrophages to hypoxia caused by enzymatic oxidation of glucose in the medium. When a glucose/glucose oxidase solution is added into the cell medium, glucose oxidase catalyzes the oxidation of glucose. This enzymatic oxidation reaction consumes molecular oxygen. The rate of the oxidation and the steady-state level of oxygen in the medium depend on the glucose concentration and glucose oxidase activity. Figure 6 describes the response of cells to hypoxia caused by different concentrations of glucose/glucose oxidase. The response is observed by monitoring the signal change of Ru(byp-pyr)$(bpy)_2$-containing lipobeads in the macrophages. Curve c is the control experiment, conducted in a glucose- and glucose oxidase-free solution. It shows that the signal of lipobeads remains constant in the absence of glucose and glucose oxidase throughout the experiment. Curves a and b describe the cellular response of macrophages to 1.5 mM glucose with 5 units/mL glucose oxidase and 2.5 units/mL, respectively, in the solution. A 40 (a) and 30% (b) fluorescence increase is obtained in 4 min, indicating a decrease in the oxygen level in the intracellular lysosomes to 4 and 4.8 ppm, respectively. It is interesting to note that the variation between the fluorescence of the lipobeads in different cells increases with decreasing oxygen level. This results in an unusual situation where the error in the experiments increases with an increase in the fluorescence signal and signal-to-noise ratio. The number of dead cells increases with decreasing oxygen concentration. The large variation in the fluorescence of the lipobeads in cells under conditions of extreme hypoxia may be attributed to a difference in their fluorescence intensity in viable and dead cells. When the glucose/glucose oxidase solution is replaced with a PBS solution at pH 7.4 10 min after the start of the enzymatic reaction, the fluorescence intensity of the lipobeads drops back to its original value in ∼5 min, indicating that a normal intracellular oxygen level has been restored. Trypan Blue staining shows that ∼85% of the cells survive this treatment. However, when the glucose/glucose oxidase solution is replaced with a PBS solution at pH 7.4 20 min after the start of the enzymatic reaction, only 50% of the cells survive these conditions of hypoxia.

The oxygen-sensitive lipobeads are also applied to assess the effect of the oxidative agent menadione on the intracellular oxygen level in macrophages. Menadione is known to generate a large quantity of ROS when it enters cells.[27] It is believed that the semiquinone radicals that are generated through the one-electron reduction of quinines can rapidly reduce dioxygen to form superoxide anion radicals and, subsequently, hydrogen peroxide,

(27) Thor, H.; Smith, M. T.; Hartzell, P.; Bellomo, G.; Jewell, S. A.; Orrenius, S. *J Biol Chem*, **1982**, *257*, 12419−12425.

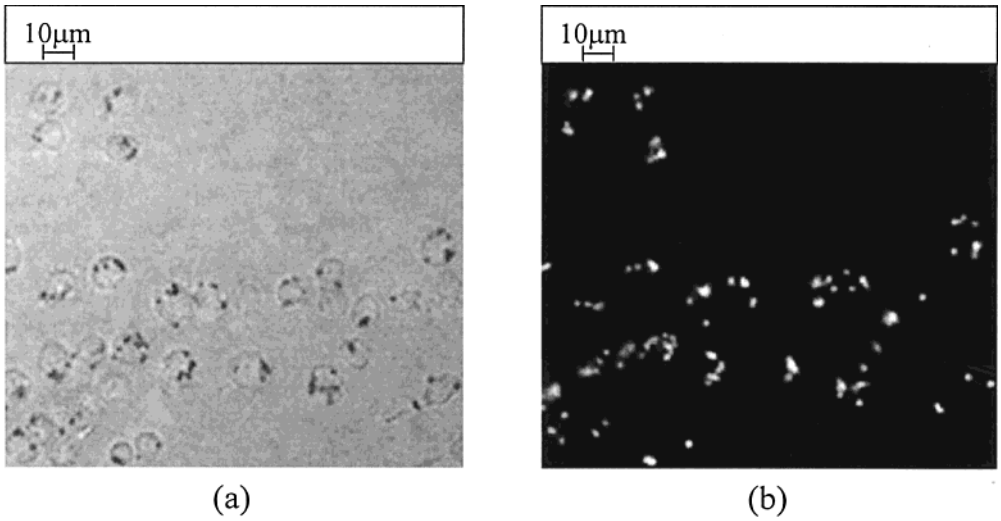

Figure 5. Phagocytosis of 2.1-μm [$(bpy)_2Ru(bpy\text{-}pyr)$] lipobeads. (a) A transmission image; (b) a digital fluorescence image of lipobeads internalized by macrophages. Objective: 40× with NA = 0.9.

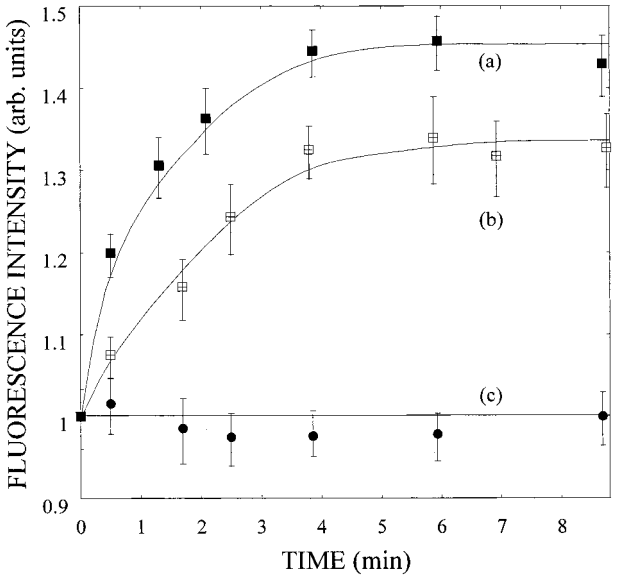

Figure 6. Intracellular oxygen level changes monitored by Ru(bpy-pry)$(bpy)_2$-containing lipobeads in macrophages. Curves a and b describe the response of the Ru(bpy-pry)$(bpy)_2$ lipobeads to a solution containing 1.5 mM glucose and (a) 2.5 and (b) 5 units/mL glucose oxidase. Curve c is a control experiment in a glucose/glucose oxidase-free solution. Error bar, 4%.

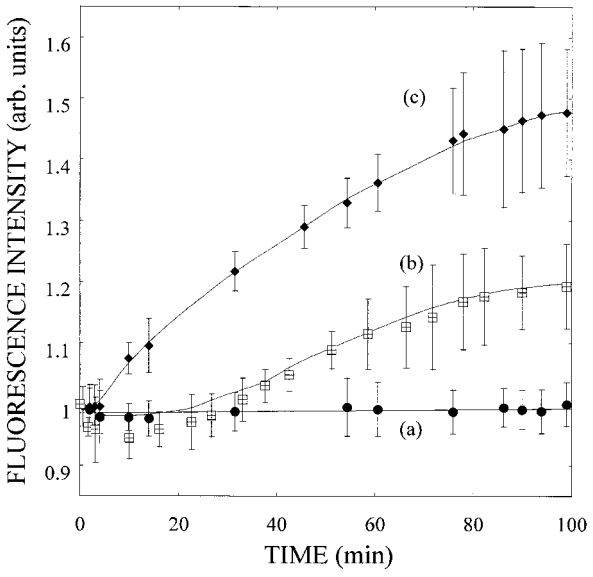

Figure 7. Response of $(bpy)_2Ru(bpy\text{-}pry)$ lipobeads in macrophages to oxygen level changes induced by menadione. Curve a is the control experiment. The cells are incubated in PBS at pH 7.4 in the absence of menadione. Curves b and c describe the response of the lipobeads to solutions containing (b) 500 μM and (c) 1 mM menadione.

hydroxyl radical, and other ROS.[27,28] Because of its prooxidant quality, menadione is often used to induce oxidative stress and study its effect on cells. Figure 7 describes the fluorescence intensity of lipobeads internalized in macrophages when the cells are exposed to the oxidizing agent menadione. Curve a is a control experiment showing that the fluorescence intensity of the lipobeads remain constant in a menadione-free solution. Curves b and c describe the fluorescence intensity of the internalized lipobeads when the cells are exposed to 1 (b) and 0.5 mM (c) menadione solutions. When the cells are exposed to 1 mM menadione, the fluorescence intensity of the lipobeads increases by 50% in ~2 h, indicating a decrease of the intracellular oxygen level to ~3.2 ppm. Treatment of the cells with 500 μM menadione results in a lower and slower change in the fluorescence intensity of the lipobeads. The decrease in oxygen level in the cells results from reduction of molecular oxygen by semiquinone radicals to form ROS. This leads to an increase in the fluorescence intensity of the lipobeads.

To evaluate the necessity of protecting the dye by immobilization in the phospholipid coating of the particles, we also measured the effect of menadione on cells loaded with free Ru(bpy-pyr)-$(bpy)_2$. We observed a 2-fold decrease in the fluorescence of the oxygen-sensitive dye when the cells were exposed to 1 mM menadione. Removal of menadione restored the signal of the dye to ~80% of its original value (data not shown). This experiment supports our prediction that, without protection, the sensing dye is prone to be affected by a variety of interfering species. In this case, the targeted agent itself, menadione, quenches the fluorescence intensity of the dye and leads to its partial degradation.

(28) DeGroot, H.; Littauer, A. *Free Radical Biol. Med.* **1989**, *6*, 541−551.

SUMMARY AND CONCLUSIONS

Oxygen-sensitive fluorescence lipobeads were prepared and used for the first time for intracellular oxygen measurements. A new oxygen indicator, Ru(bpy-pyr)$(bpy)_2$, was chosen as the oxygen indicator because of its high hydrophobicity, high oxygen sensitivity, large Stoke shift, and high photo- and chemical stability. The fluorescence intensity of single oxygen-sensing lipobeads in nitrogenated solutions was 3 times higher than their fluorescence in oxygenated solutions. The oxygen-sensitive lipobeads enabled us to monitor noninvasively and in real time the level of molecular oxygen in cells. We were also able to monitor the kinetic response of murine macrophages to hypoxia induced by the enzymatic oxidation of glucose by glucose oxidase and to oxidative stress applied by the oxidative agent menadione. Moreover, we were able to monitor these processes in a large number of cells simultaneously. Our studies show that the protection of the oxygen-sensitive fluorescence indicator is necessary to prevent its destruction or false readings because of interaction of the indicator with cellular macromolecules or ROS. Fluorescent-sensing lipobeads offer significant improvement in analytical properties compared to previously used particle-based intracellular sensors. The charge properties of the particles are easily controlled to prevent aggregation. The unique hydrophobic core−hydrophilic shell structure enables the use of hydrophobic indicators in aqueous samples. The dye molecules are protected from the cellular environment by a membrane rather than being bound or adsorbed to the surface or the bulk of the particles. This shortens the response and recovery time of the particles. Currently, we are developing fluorescence-sensing lipobeads for glucose and for zinc and calcium ions. Fabrication of lipobeads through covalent attachment between the phospholipid membrane, the indicator, and the core surface of the particles is also being developed in our laboratory.

ACKNOWLEDGMENT

This work is supported by the National Science Foundation through CAREER grant CHE-9874498. The authors thank Dr. Russell Schmehl from Tulane University Department of Chemistry for providing us with the oxygen indicator Ru(bpy-pyr)$(bpy)_2$. The authors also thank Tom Weise from Xavier University of Louisiana School of Pharmacy for the use of his cell culture laboratory.

Received for review March 21, 2001. Accepted May 24, 2001.

AC010344N